

Delving Deeper Into Astromorphic Transformers

Md Zesun Ahmed Mia,¹ Malyaban Bal,¹ Abhronil Sengupta¹

¹ The Pennsylvania State University
zesun.ahmed@psu.edu, mjb7906@psu.edu, sengupta@psu.edu

Abstract

Preliminary attempts at incorporating the critical role of astrocytes - cells that constitute more than 50% of human brain cells - in brain-inspired neuromorphic computing remain in infancy. This paper seeks to delve deeper into various key aspects of neuron-synapse-astrocyte interactions to mimic self-attention mechanisms in Transformers. The cross-layer perspective explored in this work involves bio-plausible modeling of Hebbian and pre-synaptic plasticities in neuron-astrocyte networks, incorporating effects of non-linearities and feedback along with algorithmic formulations to map the neuron-astrocyte computations to self-attention mechanism and evaluating the impact of incorporating bio-realistic effects from the machine learning application side. Our analysis on sentiment and image classification tasks on the IMDB and CIFAR10 datasets underscores the importance of constructing Astromorphic Transformers from both accuracy and learning speed improvement perspectives.

Introduction

Astrocytes, a type of glial cell, play a critical role in brain function encompassing various processes such as homeostasis, metabolism, and synaptic regulation (Perez-Catalan, Doe, and Ackerman 2021). Astrocytes detect and regulate synaptic activity in the tripartite synapse through interactions with pre and postsynaptic neurons. Investigating their impact on neural computation is currently an active research field in neuroscience and underscores the critical need to move beyond the neuro-synaptic perspective of current Artificial Intelligence (AI) systems. Recent experimental findings on neuron-astrocyte interactions and modulation have led to significant progress in computational neuroscience, enabling the development of models that incorporate neuron-astrocyte interactions within neural networks (Manninen, Aćimović, and Linne 2023; Wakida et al. 2020). Astrocytes have been found to modulate bursting in neural circuitry through the release of gliotransmitters, which have an impact on neuronal excitability and synaptic plasticity (Durkee et al. 2021; Lenk et al. 2020). Astrocytes possess the ability to encode information through calcium signaling and regulate information processing, thereby actively engaging in neural computation at the tripartite synapse level. Additionally, astrocytes possess inherent capacity as memory components (Tsybina et al. 2022; Gordleeva et al. 2022) and

plasticity regulators that are capable of facilitating local sequential learning (Gibbs, Hutchinson, and Hertz 2008; Alberini et al. 2018).

Preliminary attempts at incorporating the critical role of astrocytes in brain-inspired neuromorphic computing has started in earnest. Neuromorphic systems (Sengupta et al. 2019) are bio-plausible AI models that attempt to emulate neuronal and synaptic operations with a higher degree of bio-fidelity to tap into the huge energy efficiency of the brain. Such systems are temporal and event-driven where computation occurs through transmission of sparse spiking events between neurons - thereby offering the potential of orders of magnitude power efficiency when implemented on neuromorphic platforms (Davies et al. 2021). However, astromorphic computing encapsulating features of astrocytic regulation in neuromorphic systems still remain in infancy with works primarily targeting integration of astrocyte functionality with Spike-Timing-Dependent-Plasticity (STDP) mechanisms (Liu et al. 2018; Rastogi et al. 2021a; Han, Islam, and Sengupta 2022; Liu et al. 2017) - an unsupervised learning framework that remains limited to shallow networks and simple tasks (Diehl and Cook 2015). Other attempts also suffer from the pressing issue of scalability to complex tasks (Han, Pan, and Liu 2023).

This work is based on a recent study (Kozachkov, Kastanenko, and Krotov 2023) that has shown promise at emulating the self-attention mechanism in transformers (Vaswani et al. 2017) using a simple two layered network involving neuron-astrocyte interactions. The ability to design Astromorphic Transformers is therefore highly relevant in the current era of Large Language Models (LLMs), such as BERT (Devlin et al. 2018) and GPT (Radford et al. 2018) - paving the pathway for designing explainable transformers from a neuroscience perspective as well as addressing scaling challenges for utilizing the computational role of astrocytes in neuromorphic computing. However, as we illustrate in this work, prior work has neglected various key aspects of *bi-directional astrocytic signalling, feedback and non-linear temporal behavior* - all of which are key to address the fundamental mapping of self-attention mechanism to astrocyte-neuron interactions along with providing insights on whether such intrinsic non-linear dynamics and plasticity modulation enable better learning capabilities from the application side. The distinguishing feature of this work

therefore lies in the **neuroscience-algorithm-application co-design** perspective seeking to answer the following questions: **(i) Theoretical neuroscience:** What aspects of astrocyte functionality should be included in neural architectures to better explain self-attention mechanism in transformers? **(ii) Algorithm:** Can we map key algorithmic modules like relative positional information encoding of tokens to astrocytic interactions by drawing qualitative inspiration from theoretical neuroscience? **(iii) Application:** What is the impact of incorporating such dynamic temporal bio-plausible transformers from the machine learning application perspective?

Related Works and Main Contributions

Understanding the role of astrocytes in neuromorphic computing, especially from the algorithm perspective, is relatively nascent. While hardware implementation of astrocyte functionality in CMOS (Ranjbar and Amiri 2015; Karimi et al. 2018) as well as post-CMOS technologies (Garg, Yang, and Sengupta 2021) have been explored, algorithm level works exploiting the role of astrocytes and leveraging their computational role has largely remain limited to self-repair functionality of faulty neural network hardware (Wade et al. 2012a; Liu et al. 2018; Rastogi et al. 2021b; Han, Islam, and Sengupta 2022). This is mainly inspired by the fact that astrocytes, through their synaptic plasticity regulation and feedback mechanisms, enable neurons to fire at a baseline ideal frequency. This property can be utilized to mitigate neuromorphic hardware non-idealities with stuck-at-faults and drift effects (Han, Islam, and Sengupta 2022). However, such approaches are still limited to single layered unsupervised networks where astrocyte functionality is integrated with STDP learning mechanisms.

Recent studies have also examined the influence of astrocytes on learning (Alberini et al. 2018), working memory (Tsybina et al. 2022), energy minimization in neural networks (Fountain and Merkel 2022), robotic locomotion control (Polykretis, Tang, and Michmizos 2020), structure learning (Han, Pan, and Liu 2023), among others.

Building upon recent works (Kozachkov, Kastanenka, and Krotov 2023) at emulating self-attention module in transformers through astrocyte-neuron interactions, we develop a computational framework that encapsulates key aspects of temporal non-linearities and feedback enabled by astrocytes and underscore the importance of incorporating such bio-plausible effects through a comprehensive evaluation of Astromorphic Transformers on a benchmark evaluation set. Our work expands the computational capabilities of astrocyte-neuron network architectures equipped with plasticity, for the first time, to a broad category of sequential tasks.

Results

Transformers

Vanilla transformers (Vaswani et al. 2017) for classification tasks usually consist of an encoder block processing the provided $key(K)$, $query(Q)$ and $value(V)$ generated from the

input token embeddings X (words in language tasks, pixels in vision tasks, etc.). Appendix A in the supplementary material illustrates the conventional configuration of a transformer, featuring a block referred to as “Multi-Head Attention” that produces the contextual association among the provided inputs. The Multi-Head Attention block in transformers uses self-attention mechanisms for multiple input heads, allowing the model to allocate varying importance to individual tokens, focusing on salient features for precise output in specific contexts.

The transformer implements auto-regressive attention by computing the dot product of key and $query$, and then multiplying the resulting scalar with the corresponding $value$ derived from the input token. Implementing the softmax function (a type of distribution function) atop the dot product of key and $query$ (to enforce attention over the tokens) increases the order of complexity, a predicament that can be alleviated by the use of linearized attention (Schlag, Irie, and Schmidhuber 2021). Linearized attention exploits the distributive property of matrix multiplication resulting in lower complexity for self-attention computation. More details can be found in Appendix B of the supplementary material. From the linear attention-based transformer (linear transformer) perspective (Katharopoulos et al. 2020), the transformer equations can be defined in the following form:

$$SA(X) = \frac{\phi(Q)(\phi(K)^T V)}{\phi(Q)[\sum_{t=1}^{t=N} \phi(k_t)]^T} \quad (1)$$

$$Y = \text{LayerNorm}(SA(X) + X) \quad (2)$$

$$Z = \text{Softmax}(\text{Linear}(\text{LayerNorm}(\text{FFN}(Y) + Y))) \quad (3)$$

From Equations 2 and 3, we can see that the output of self-attention is Y , which undergoes layer normalization after being augmented with residual connections from the input layer. The transformer determines the final output probabilities, denoted by Z . There is a $\phi(\cdot)$ feature map that corresponds to a positive similarity function. When two such functions are multiplied, the normalized dot product maps to a distribution function (Chaudhari et al. 2021) (i.e. softmax). According to (Katharopoulos et al. 2020), $\phi(\cdot)$ can be defined by Equation 4. Here, the activation function $elu(x)$, which stands for exponential linear unit, is utilized for efficient and precise learning (Clevert, Unterthiner, and Hochreiter 2015).

$$\phi(x) = elu(x) + 1; \quad (4)$$

In the next section, we discuss the tripartite synapse model and aspects which will be necessary in constructing astromorphic transformers.

Tripartite Synapse Dynamics

Astrocytes play a crucial role in the modulation of synaptic plasticity by releasing chemical signals that regulate the efficacy of synaptic connections. This phenomenon plays a role in modulating the strength and duration of synaptic connectivity and is crucial for maintaining the health of neurons. The depiction of the tripartite synapse in Fig. 1, which incorporates astrocytes, is a biologically plausible representation that embodies a multifaceted and evolving comprehension of synaptic signaling within the brain.

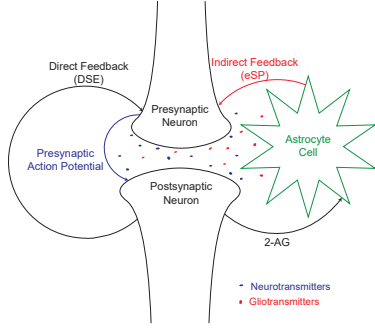


Figure 1: A model of synaptic communication in the brain. The tripartite synapse consists of presynaptic neurons, postsynaptic neurons and astrocytes. Astrocytes detect neuronal activity and respond bidirectionally by emitting gliotransmitters, thereby modulating the intensity and duration of synaptic communication.

Astrocyte dynamics: The tripartite synapse’s dynamics are based on Li and Rinzel Ca^{2+} dynamics (Li and Rinzel 1994), gatekeeper model (Volman, Ben-Jacob, and Levine 2007), Nadkarni and Jung model (Nadkarni and Jung 2004, 2007), and bidirectional study on astrocytic glutamate binding to postsynaptic neurons (AN model) (Wade et al. 2011). According to the biophysical models, it is observed that an action potential (AP) is generated by the presynaptic axon through the release of neurotransmitters. Neurotransmitters bind to postsynaptic dendrites, causing depolarization. This leads to the release of 2-Arachidonylglycerol (2-AG) from postsynaptic neurons to type 1 Cannabinoid Receptors (CB1Rs) on the presynaptic terminal. This process is called Depolarization-induced Suppression of Excitation (DSE) and depresses the continuous release of neurotransmitters by inhibiting presynaptic neurons (Alger 2002). Neurotransmitter release also involves binding 2-AG to CB1Rs on an astrocyte, enveloping the synapse and increasing Inositol 1,4,5-trisphosphate (IP_3) levels. IP_3 facilitates the release of calcium ions into the cytoplasm, thereby, increasing calcium concentration. Three currents, $J_{channel}$, J_{leak} , and J_{pump} , are introduced to model the rate of change of calcium concentration inside the astrocyte (Li and Rinzel 1994). When calcium concentration crosses a threshold, astrocytes discharge glutamate, which binds to presynaptic group I metabotropic Glutamate Receptors (mGluRs), creating a process called eSP (Indirect Feedback) from the astrocyte to the presynaptic neuron (Navarrete and Araque 2010). The comprehensive description of the computational model (Equation 5 introduces the basic equation of the model) can be found in the works of (Wade et al. 2012b, 2011; De Pittà et al. 2009).

$$\frac{d(Ca^{2+})}{dt} = J_{channel} + J_{leak} - J_{pump} \quad (5)$$

Neuron dynamics: In this work, we consider the passive Leaky Integrate and Fire (LIF) dynamics to describe the neu-

ron firing process, which is described as follows:

$$\tau_m \frac{dv}{dt} = -v(t) + R_m \sum_{i=1}^M I_{total-syn}^i \quad (6)$$

where, τ_m represents the membrane time constant, v represents the membrane potential, and R_m represents the membrane resistance. $I_{total-syn}^i$ denotes the total synaptic current at the i^{th} synapse. M is the number of synapses connecting to the corresponding neuron. Total synaptic current at the i^{th} synapse can be defined as the summation of two currents namely, Synaptic Current, I_{syn}^i and Slow Inward Current, $SIC(t)$ in Equation 7:

$$I_{total-syn}^i = I_{syn}^i + SIC(t) \quad (7)$$

I_{syn}^i is the intrasynaptic current which varies linearly with the amount of neurotransmitters present in that synapse at any time, t ($I_{syn}^i = A_{se} y_i(t)$ where, A_{se} and $y_i(t)$ represent the absolute synaptic efficacy and the amount of neurotransmitter discharged by the synapse at a given time t , respectively). Thus, I_{syn}^i depends on the direct feedback (corresponds to DSE) as direct feedback is modulated by the amount of neurotransmitters between the pre and postsynaptic neuron. On the other hand, the extrasynaptic Slow Inward Current ($SIC(t)$) is generated when astrocyte-released glutamate interacts with extrasynaptic NMDARs (located in postsynaptic neuron) (Haydon and Carmignoto 2006). To elaborate, the activation of astrocytes leads to the release of glutamate from these cells. Upon its release, glutamate interacts with NMDARs located on the postsynaptic neuron, resulting in the emergence of a distinct form of current known as Slow Inward Current ($SIC(t)$) (Wade et al. 2011). The details of the mathematical modeling of $SIC(t)$ can be found in (Wade et al. 2011).

Next, we develop a network architectural framework to mimic the self-attention mechanism in transformers using the astrocyte and neuron dynamics described herein and evaluate the impact of inherent non-linearities and feedback.

Neural Network Emulating Self-Attention

Self-attention is a fundamental component of all transformer models. Based on prior works of mimicking self-attention by astrocytes (Kozachkov, Kastanenka, and Krotov 2023), we adopt a network topology as shown in Fig. 2. The neural network architecture comprises three distinct layers, namely the Input layer, Hidden layer, and Output layer. There exists two distinct operational modes for the aforementioned neural network: (i) write mode and (ii) read mode. Upon presentation of the tokens ($x_t \in R^{1 \times d}$: which may include word embeddings and image embeddings) to the input layer, the write mode is initially employed, followed by the read mode to generate the outputs. In write mode, we encode information into the network by means of *keys* and *values*, whereas, in read mode, we retrieve the information by providing *queries*.

During the write mode, the input layer sequentially transmits the *keys* ($k_t = x_t W_K$; $W_K \in R^{d \times m}$) for each token to the hidden layer and the *values* ($v_t = x_t W_V$; $W_V \in R^{d \times d}$)

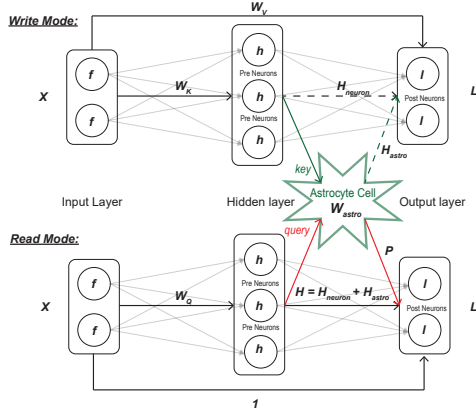


Figure 2: The neural network architecture showing the three layers. As tokens are presented to the network as a d dimensional vector, there are d neurons in both the input and output layers. Hidden layer has m neurons. Solid lines indicate active operations, therefore H_{neuron} and H_{astro} are learnt during write mode but utilized during read mode.

to the output layer. The hidden layer neurons introduce a nonlinearity within the system by activating a feature map, denoted as $\phi(\cdot)$, on the transmitted *keys*. Use of $\phi(\cdot)$ reduces the computational complexity and memory usage inspired from linearized attention mechanism. More information on the reduction of the order of complexity is discussed in Appendix B (with Fig. S2 illustrating the idea) in the supplementary material. A presynaptic neuron in the hidden layer is intricately connected with an astrocyte and an output layer neuron, forming a tripartite synapse. Similar to the mechanism by which the presynaptic neuron stimulates the astrocyte through the release of neurotransmitters, in this context, the astrocyte is being activated through the transmission of *keys* from neurons in the hidden layer. The write mode can be mathematically expressed as in Equation 8:

$$\begin{aligned} f_t &= x_t \\ h_t &= \phi(f_t W_K) = \phi(k_t) \\ l_t &= f_t W_V = v_t \end{aligned} \quad (8)$$

In order to establish the read mode equations, it is necessary to first formulate the neural plasticities that occur among the components of the tripartite synapse. Moreover, our work aims at exploring strong bio-plausible correlations at modelling such plasticities, which ultimately influence our neuroscience-algorithm-application co-design analysis. In a subsequent section, we will examine the read mode which is responsible for retrieving the encoded information.

Mathematical Formulation of Plasticity

(i) Hebbian Plasticity: Hebbian plasticity is characterized by the sequential adjustment of synaptic weights in accordance with the interconnection pattern between two neurons (pre and postsynaptic neurons) at the synapse. Previous studies (Kozachkov, Kastanenko, and Krotov 2023) have exclusively focused on the plasticity occurring between two neu-

rons neglecting non-linearities and the plasticity that may occur between astrocytes and postsynaptic neurons, which is also involved in the learning process.

Contribution I: In the context of Hebbian plasticity, we underscore the importance of addition of astrocyte-postsynaptic neuron connected Hebbian-inspired learning along with inherent non-linearities. To elaborate, the synaptic weights (H_{neuron}) that establish connections between the presynaptic and postsynaptic neurons are acquired through Hebbian plasticity during the write mode. This learning occurs due to the connection between pre and postsynaptic neuron which can be mapped to the synaptic current (I_{syn}) from the neuroscience perspective. As discussed previously, I_{syn} is modulated by DSE so, H_{neuron} is inspired from the *direct feedback* in the tripartite synapse. This leads to Hebbian plasticity between the hidden layer (presynaptic neuron) and the output layer (postsynaptic neuron). Hidden neuron outputs are denoted as $h_t = \phi(k_t)$ whereas the output (last) layer outputs are denoted as $l_t = v_t$ in the write mode (refer to Equation 8). H_{neuron} weights are learnt via Equation 9, where m acts as a scaling factor affecting the learning speed.

$$H_{neuron,t} = H_{neuron,t-1} + \frac{1}{m} h_t^T l_t \quad (9)$$

The astrocyte functions as the third constituent in the tripartite synapse, enabling bidirectional communication with the synaptic neurons. Hence, we propose that the connection between the astrocyte and the postsynaptic neuron be also represented in this formulation through a learnable weight matrix (H_{astro}), in accordance with the Hebbian rule. Equation 10 shows the learning mechanism of these weights in which the presynaptic neuron output (h_t) is replaced by the astrocytic activity, represented by W_{astro} , as this connection incorporates the astrocyte and the postsynaptic neuron. The formulation of W_{astro} will be considered in the succeeding text.

$$H_{astro,t} = H_{astro,t-1} + \frac{1}{m} W_{astro} l_t \quad (10)$$

The weight, denoted as H_{astro} , is inspired from the extrasynaptic current *SIC* (refer to tripartite synapse dynamics section). According to Equation 7, *SIC* is added to I_{syn} to generate the total synaptic current. Consequently, the two distinct learnable weights, denoted as H_{neuron} and H_{astro} , are combined to produce the Hebbian weight $H = H_{neuron} + H_{astro}$.

Astrocytes have a significant impact on the Hebbian weight due to their inherent non-linearity. A recent study by (Han, Pan, and Liu 2023) introduced an AstroNet model that optimizes neural network connections through temporal and global regulation mechanisms. The authors found that astrocytes introduce non-linear effects, which compound the pre-existing nonlinearity of neurons. The concept of Hebbian Plasticity is associated with temporal and global regulation, where the current weight is influenced by past neuron weights and astrocytic weights. To map the effect of non-linearity, we consider that the summation of neuron and astrocyte Hebbian weights undergoes non-linear activation, ultimately generating the Hebbian weight (H). As such, we

propose the integration of a sigmoid (σ) nonlinearity into the learning process. Thus, the weight H exhibits the collective Hebbian plasticity of a tripartite synapse, as elucidated by Equation 11, where K and V correspond to *keys* and *values* of all the N tokens in a single sequence (in matrix form: $K \in \mathbb{R}^{N \times m}$, $V \in \mathbb{R}^{N \times d}$). Assuming initial $H_{neuron,0}$ and $H_{astro,0}$ from Equations 9 and 10 are both zero, we can define the Hebbian weight in its matrix form (H) as,

$$H = \sigma(H_{neuron} + H_{astro})$$

$$H = \sigma\left(\frac{1}{m}(\phi(K)^T V + W_{astro} * V)\right) \quad (11)$$

Next, we consider formulation of the astrocytic activity parameter, W_{astro} . We note that astrocytic Ca^{2+} dynamics is a relatively slower temporal process than the streaming rate of the input tokens. Therefore, it is expected that the astrocytic activity should encode relative information among successive tokens. In this context, we derive inspiration from algorithmic formulations of relative positional information of tokens, popularly used in Vision transformers (Shaw, Uszkoreit, and Vaswani 2018; Ramachandran et al. 2019), and map it to the activity parameter W_{astro} . The astrocytic response parameter is therefore defined to use the edge of the tokens to capture relative position differences between input elements (Shaw, Uszkoreit, and Vaswani 2018). The edge of the tokens considers the pairwise relationships between input elements in the sense that the input is modeled as a labeled, directed, fully-connected graph. The edges pertaining to relative positional information are learnt using the temporal regulation property of astrocytes through the activity parameter, W_{astro} . Consequently, H_{astro} can be considered as a representation of acquired positional knowledge derived from the input tokens. W_{astro} can be modeled using Equation 12 where, a_{ij} is the edge between input tokens x_i and x_j .

$$W_{astro} = \phi(a_{ij})^T \quad (12)$$

(ii) Presynaptic Plasticity: The plasticity resulting from the induced calcium response inside the astrocyte due to bidirectional communication between the astrocyte and presynaptic neurons (hidden layer) can be defined as presynaptic plasticity. As tokens are sequentially presented to the hidden layer during the write mode, *keys*: $\phi(k_t)$ are generated which can be mapped to an increasing number of released neurotransmitters (implying increment in $J_{channel}$ as per the computational neuroscience model), thereby resulting in elevation of the calcium concentration within the astrocyte (evident from Equation 5). Thus, presynaptic plasticity parameter g , can be mapped to calcium concentration in astrocytes modulated by indirect feedback (*eSP*), and can be expressed as the aggregate of the inputs ($h_t = \phi(k_t)$) received by the presynaptic neuron. Equation 13 defines the formulation of the presynaptic plasticity parameter (g). Assuming the initial calcium concentration to be zero ($g_0 = 0$), g can be expressed as,

$$g_t = g_{t-1} + h_t = g_{t-1} + \phi(k_t) \quad (\text{pertoken form})$$

$$g = \sum_{t=1}^N \phi(k_t) \quad (\text{matrix form}) \quad (13)$$

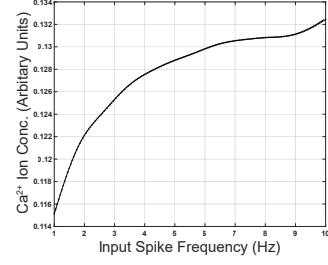


Figure 3: As the input spike frequency in the presynaptic neurons increases, the rate of increase in calcium concentration slows down, thereby exhibiting a non-linear relationship between Ca^{2+} ion concentration and input spike rate.

Contribution II: Prior work (Kozachkov, Kastanenka, and Krotov 2023) at modelling pre-synaptic plasticity has not considered the intrinsic non-linear Ca^{2+} dynamics of the astrocytes in response to increasing firing rate of presynaptic neurons. Due to the indirect feedback (*eSP*), the rate of increase in the release rate of neurotransmitters gradually reduces in response to an increase in presynaptic neuron firing over time. Hence, a non-linear relationship exists between the calcium concentration and the frequency of spikes received from the presynaptic neuron. We substantiate this observation by simulating the AN model (Wade et al. 2012b, 2011). The associated non-linear variation is depicted in Fig. 3 which leads us to modify the presynaptic plasticity parameter g as,

$$g = \left(\sum_{t=1}^N \phi(k_t)\right)^\alpha \quad (14)$$

where, the exponent α encodes the degree of non-linearity. From our computational modelling, we use a value of $\alpha = 0.25$. The subsequent section elaborates on the read mode operation which involves the process of retrieving the information encoded during the write mode to implement self-attention mechanism incorporating our key contributions towards more bio-plausible formulations of Hebbian and presynaptic plasticity.

Realization of Self-Attention

Self attention mechanism is realized when the encoded information is accessed during the read mode to obtain the activations of the output layer neurons. The hidden layer neurons receive *queries* ($q_t = x_t W_Q$) from the input layer and access the information that was previously encoded within the astrocyte. This information is stored via both the Hebbian weight (H) and the presynaptic plasticity parameter (g) during write mode. However, during read mode, H is already learnt and not modulated by the transmitted *queries* from the presynaptic neurons as it is directly connected to the postsynaptic neurons (output layer). As g is the presynaptic plasticity parameter, it has no direct connection to the postsynaptic neuron. Therefore, the information encoded in g has to be retrieved by the *queries* transmitted from the hidden layer during read mode by inducing a calcium response from the astrocytes. In order to read the calcium response

(c_t) of the astrocyte, the *queries* (h_t) are scaled by the corresponding presynaptic plasticity parameters (g_t) across all the m hidden neurons and then summed together. This is depicted in Equation 15, where the matrix form of the calcium response is defined by C .

$$c_t = \sum_m g_t h_t \quad (\text{pertoken form})$$

$$C = hg^T \quad (\text{matrix form}) \quad (15)$$

Let us define the weight modulating the connection between the astrocyte and the output layer as P . According to studies regarding Tumor Necrosis Factor - α ($TNF - \alpha$), astrocytes possess the ability to boost synaptic weights in reaction to low neural activity and diminish weights in reaction to high neural activity (Kozachkov, Kastanenko, and Krotov 2023) by means of calcium response (neural activity is proportional to released neurotransmitters). Consequently, it is possible to infer an inverse correlation between P and the calcium response (C). Simplifying, this relation is given by,

$$P = \frac{1}{\phi(Q)((\sum_{t=1}^N \phi(k_t))^\alpha)^T} \quad (16)$$

Given that the presynaptic plasticity modulated weight (P) is ascertained, we can define the network equations for the read mode. As seen from Fig. 2, the hidden layer and the output layer are connected by the Hebbian weight H and the astrocyte is imposing another learnt weight (from calcium response) denoted by P onto the existing weight H . Thus the weights are implemented by the Hadamard multiplication (element-wise: \odot) of H and P onto the output layer. Furthermore, the output layer receives the input (F) directly from the input layer modulated by unity weight to implement the residual connection present in the self-attention module of transformers. Considering the network architecture, the read mode network equations can be defined in Equation 17. It is important to highlight here that during the read mode, the decoding process occurs in a singular timestep, as opposed to the sequential nature of the write mode. Hence, all the parameters for input, hidden and output layers are represented in their matrix format.

$$F = X$$

$$h = \phi(FW_Q) = \phi(Q) \quad (17)$$

$$L = h \times (H \odot P) + F = \phi(Q)(H \odot P) + F$$

In Equation 17, all the parameters are in matrix mode, where the dimensions are defined as follows: $W_Q \in R^{d \times m}$, $X \in R^{N \times d}$ (input tokens) and $Q \in R^{N \times m}$ (queries). L represents the generated output from the last layer. Self-attention algorithm is defined when the network completes a write and read mode as discussed next.

By substituting the values of H and P from Equation 11 and 16 into Equation 17, the resulting Equation 18 can be obtained after the write and read mode:

$$L = \frac{\phi(Q)(\sigma(\phi(K)^T V + W_{astro} V))}{m \times \phi(Q) \sum_{t=1}^N [\phi(k_t)^\alpha]^T} + X \quad (18)$$

In Equation 18, L implements identical operation as the transformer self-attention from Equation 1 (along with the

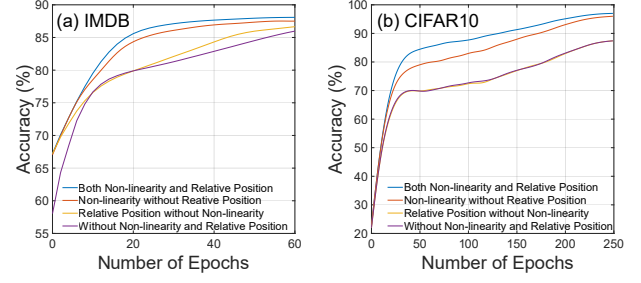


Figure 4: Comparative analysis to examine the effects of incorporating non-linearity and relative positional encoding in the astromorphic transformer on the (a) IMDB and (b) CIFAR10 datasets. The yellow and purple lines in Fig. (b) are nearly overlapping.

inclusion of an extra residual connection from the input layer). Thus, with this implementation, the astromorphic transformer is formulated.

Performance Evaluation

Our astromorphic transformer is trained and tested on two different tasks. These include sentiment classification on the IMDB dataset (Maas et al. 2011) and image classification on the CIFAR10 dataset (Krizhevsky and Hinton 2009). Methods section discusses the hardware specifications, datasets and model architectures while Appendix C in the supplementary material lists all the associated hyper-parameters.

To date, there has not been any language or vision model that incorporates transformer architecture in a manner that is bioplausible and derived from neuron-astrocyte interactions. We report an accuracy of $88.7 \pm 0.2\%$ for the sentiment classification task on the IMDB dataset, utilizing the non-linearity and relative positional information in the model. We also achieve $97.0 \pm 0.2\%$ accuracy using an astromorphic vision transformer on the CIFAR10 dataset.

Table 1 compares performance of our astromorphic transformer against neuromorphic as well as other non-bioplausible models on the IMDB and CIFAR10 datasets. Our model outperforms RNNs, LSTMs, and GRUs on the IMDB dataset and other bioplausible neuromorphic architectures. However, we did not compare with existing pretrained transformers (BERT, GPT, etc.) because these models are pretrained using non-bioplausible self-attention and have customized pretrained learnable embeddings for natural language processing, whereas we use fixed GloVe embeddings (Pennington, Socher, and Manning 2014) that are simple enough to implement in our astromorphic attention-based transformer architecture. We also test the competitiveness of astromorphic attention in vision transformer architecture. As shown in Table 1, our astromorphic vision transformer model competes with artificial and outperforms bioplausible models on the CIFAR10 dataset.

Ablation Studies

Learning speed: The impact of the two primary contributions of our study is illustrated in Fig. 4. It is evident from

Task	Model	Neuromorphic Implementation	Bioplusibility	Accuracy
Sentiment Classification (IMDB Dataset)	Memristor SNN (Huang et al. 2023)	Directly trained in SNN domain	Yes	84.86%
	Memristor SNN (Huang et al. 2023)	Converted from ANN	Yes	85.88%
	ANN (Huang et al. 2023)	No spiking activity	No	86.02%
	Spike-transformer (Mueller et al. 2021)	Rate coded approach using Spiking Neurons	Yes	86.36%
	Recurrent SNN (Wang et al. 2022)	Presynaptic current based backpropagation	Yes	86.82%
	HRNaEMSA biGRU (Leng et al. 2021)	Implements multi-headed attention	No	87.3%
	HRNaEMSA biLSTM (Leng et al. 2021)	Implements multi-headed attention	No	87.4%
	CoRNN (Rusch and Mishra 2020)	Coupled oscillators modeled as neurons	No	87.4%
	LSTM (Aswani et al. 2021)	Memristor crossbars mimicking NN	No	87.48%
	SNN (Agrawal et al. 2021)	Compute-in-memory macro using SNN	Yes	88.15%
	UniCoRNN (Rusch and Mishra 2021)	Solves vanishing gradient problem in BPTT	No	88.4%
Transformer	Softmax attention without bioplusibilities	No	88.9 ± 0.1%	
	Astromorphic Transformer (Our Model)	Implements astromorphic attention with non-linearity and relative positional information	Yes	88.7 ± 0.2%
Image Classification (CIFAR10 Dataset)	BioLeaf (Yang and Li 2021)	SNNs trained by BP-based rules	Yes	86.88%
	STBP in CIFARNET (Zhou et al. 2023)	Spatio-temporal backprop	No	89.83%
	VGG16-SNN (Srinivasan et al. 2020)	ANN-SNN conversion	Yes	91.55%
	MS-ResNet (Hu et al. 2021)	SNN oriented ResNet-110 architecture	No	91.72%
	ANN (Zhou et al. 2022)	ResNet-19 (12.63M parameters)	No	94.97%
	ANN (Zhou et al. 2022)	Transformer-4-384 (9.32M parameters)	No	96.73%
	Spikformer (Zhou et al. 2022)	Spikformer-4-384 (9.32M parameters)	Yes	95.19%
	Spikingformer (Zhou et al. 2023)	Spikingformer-4-384 (9.32M parameters)	Yes	95.61%
	Transformer	Softmax attention without bioplusibilities	No	97.4 ± 0.1%
	Astromorphic Transformer (Our Model)	Implements astromorphic attention with non-linearity and relative positional information	Yes	97.0 ± 0.2%

Table 1: Performance comparison of our proposed astromorphic attention-based transformer architecture against other benchmarks with varying degrees of bioplusibility on the IMDB and CIFAR10 datasets.

the Fig. that the absence of relative positional information leads to a decrease in the learning speed of the model. Measuring the number of epochs to reach 85% (85%) accuracy on the IMDB (CIFAR10) dataset, we find that: (i) with both of our contributions (non-linearity and relative positional information), it takes only 16 ± 2 (45 ± 3) epochs, whereas (ii) with only the non-linearity included, it takes 22 ± 2 (111 ± 4) epochs, and (iii) with only relative positional information, it takes 43 ± 4 (215 ± 2) epochs, and (iv) without both, it takes 54 ± 4 (215 ± 2) epochs to reach the specified accuracy.

Final accuracy: We implement the theoretical model proposed by (Kozachkov, Kastanenko, and Krotov 2023) to see how it compares without the bioplusibilities proposed herein and find an accuracy of $88.0 \pm 0.2\%$ and $87.4 \pm 0.1\%$ on the IMDB and CIFAR10 datasets, respectively. This implementation does not incorporate the non-linearity and relative positional information that are integral to our model, which draws inspiration from the dynamics between neurons and astrocytes, thereby underscoring the strong need to consider such bioplusibilities in modeling astromorphic transformers. Our astromorphic transformer also competes with an iso-architecture standard non-bioplusible transformer with softmax attention (see “Transformer” entry in Table 1).

Discussion

This study aims to provide a detailed explanation of the development of an astromorphic transformer using bioplus-

ible self-attention. The inspiration for this approach is drawn from the dynamics of bidirectional communication between astrocytes and neurons in a tripartite synapse. In this study, we exploit the intrinsic Presynaptic and Hebbian plasticity of the astrocyte to incorporate two novel advancements into the transformer architecture. Subsequently, we demonstrate the effectiveness of our model on two distinct machine learning tasks. The performance of Astromorphic Transformers on sentiment and image classification tasks is presented for the first time on the IMDB and CIFAR10 datasets and is found to perform at par with an iso-architecture non-bioplusible transformer model. Implementation of Astromorphic Transformers on neuromorphic hardware has the potential of enabling scalable, robust, power and energy efficient computing paradigms that are applicable to a broad range of sequential processing tasks - a significant shift from the huge computational requirements of conventional deep learning solutions like Large Language Models.

Future research in this area could involve the exploration of astrocyte-to-astrocyte communication through gap junctions. This approach may enable the parallelization of Presynaptic and Hebbian plasticity, potentially addressing the limitation of a slower calcium response in comparison to neuron activation. In addition, it is possible to modify our model to accommodate large language models such as BERT and GPT. This can be achieved by incorporating the functionalization of relative positional information with the customized embedding of these models from a neuromorphic

perspective. Further, quantifying the energy efficiency benefits of implementing Astromorphic Transformers on neuromorphic hardware can be an area of exploration.

Methods

Hardware Specifications

The astromorphic transformer under consideration has been executed through the utilization of a GPU-based platform running PyTorch. The computational procedures were executed on a hardware configuration comprising a 12 core Intel(R) Xeon(R) Platinum 8167M CPU @ 2.00GHz, in conjunction with an NVIDIA® Tesla® V100 GPU possessing 16384 Mega Bytes of graphics memory. While simulating the model on the IMDB dataset, the model uses 1.7 GB of memory whereas it uses 4.4 GB of memory on the CIFAR10 dataset.

Dataset Details

The IMDB dataset, created by Stanford University, contains 50,000 movie reviews (each 250-500 words long) labeled as positive or negative. The data is presented in a tab-delimited format, containing fields for movie title, review text, and sentiment label. The CIFAR-10 dataset is a collection of computer vision data, comprising 60,000 color images with dimensions of 32×32 pixels. These images are categorized into 10 distinct classes, with each class containing 6,000 images. The dataset exhibits a relatively diminutive size, comprising low-resolution images and notable diversity within each class.

Network Architecture

In the Sentiment classification task, a transformer with an encoder-based architecture is employed. We use a similar architecture as depicted in the Fig. S1 with 1 encoder layer and 4 headed self-attention. We use the combination of GloVe word embeddings with one-hot positional encoding as input tokens. A dropout layer is employed after the addition of residual connection just before the layer normalization.

Meanwhile, for image classification, a convolutional and self-attention based neural network (CoAtNet (Dai et al. 2021)) was utilized to implement our proposed innovations. CoAtNet transformer architecture can best utilize the effectiveness of relative positional information when trained on vision task focused datasets. Furthermore, CoAtNet leverages the capabilities of Convolutional Neural Networks (CNNs) and transformers to enhance its performance. Our architecture implements a 3×3 convolution before creating patches from the images. We use a patch size of 2 on the image inputs and employ an 8-layered encoder stack with 8-headed self-attention. In addition to the original CoAtNet architecture, we add additional non-linearity and average pooling after encoder layers.

For both the architectures, AdamW optimizer and Cross Entropy Loss are used to learn the weights of the neural network. For IMDB dataset tokenization, we used the Glove pretrained word vectors with 840B tokens, 2.2M vocab (cased), 300D vectors.

References

- Agrawal, A.; Ali, M.; Koo, M.; Rathi, N.; Jaiswal, A.; and Roy, K. 2021. IMPULSE: A 65-nm digital compute-in-memory macro with fused weights and membrane potential for spike-based sequential learning tasks. *IEEE Solid-State Circuits Letters*, 4: 137–140.
- Alberini, C. M.; Cruz, E.; Descalzi, G.; Bessières, B.; and Gao, V. 2018. Astrocyte glycogen and lactate: New insights into learning and memory mechanisms. *Glia*, 66(6): 1244–1262.
- Alger, B. E. 2002. Retrograde signaling in the regulation of synaptic transmission: focus on endocannabinoids. *Progress in neurobiology*, 68(4): 247–286.
- Aswani, A.; Kumar, R.; Tripathi, J. N.; and James, A. 2021. Performance of Crossbar based Long Short Term Memory with Aging Memristors. In *2021 IEEE 3rd International Conference on Artificial Intelligence Circuits and Systems (AICAS)*, 1–4. IEEE.
- Chaudhari, S.; Mithal, V.; Polatkan, G.; and Ramanath, R. 2021. An attentive survey of attention models. *ACM Transactions on Intelligent Systems and Technology (TIST)*, 12(5): 1–32.
- Clevert, D.-A.; Unterthiner, T.; and Hochreiter, S. 2015. Fast and accurate deep network learning by exponential linear units (elus). *arXiv preprint arXiv:1511.07289*.
- Dai, Z.; Liu, H.; Le, Q. V.; and Tan, M. 2021. Coatnet: Marrying convolution and attention for all data sizes. *Advances in neural information processing systems*, 34: 3965–3977.
- Davies, M.; Wild, A.; Orchard, G.; Sandamirskaya, Y.; et al. 2021. Advancing neuromorphic computing with loihi: A survey of results and outlook. *Proceedings of the IEEE*, 109(5): 911–934.
- De Pittà, M.; Goldberg, M.; Volman, V.; Berry, H.; and Ben-Jacob, E. 2009. Glutamate regulation of calcium and IP 3 oscillating and pulsating dynamics in astrocytes. *Journal of biological physics*, 35: 383–411.
- Devlin, J.; Chang, M.-W.; Lee, K.; and Toutanova, K. 2018. Bert: Pre-training of deep bidirectional transformers for language understanding. *arXiv preprint arXiv:1810.04805*.
- Diehl, P. U.; and Cook, M. 2015. Unsupervised learning of digit recognition using spike-timing-dependent plasticity. *Frontiers in computational neuroscience*, 9: 99.
- Durkee, C.; Kofuji, P.; Navarrete, M.; and Araque, A. 2021. Astrocyte and neuron cooperation in long-term depression. *Trends in Neurosciences*, 44(10): 837–848.
- Fountain, A.; and Merkel, C. 2022. Effect of biologically-motivated energy constraints on liquid state machine dynamics and classification performance. *Neuromorphic Computing and Engineering*, 2(2): 024005.
- Garg, U.; Yang, K.; and Sengupta, A. 2021. Emulation of astrocyte induced neural phase synchrony in spin-orbit torque oscillator neurons. *Frontiers in neuroscience*, 15.
- Gibbs, M. E.; Hutchinson, D.; and Hertz, L. 2008. Astrocytic involvement in learning and memory consolidation. *Neuroscience & Biobehavioral Reviews*, 32(5): 927–944.

- Gordleeva, S.; Tsybina, Y. A.; Krivonosov, M. I.; Tyukin, I. Y.; et al. 2022. Situation-based memory in spiking neuron-astrocyte network. *arXiv preprint arXiv:2202.07218*.
- Han, M.; Pan, L.; and Liu, X. 2023. AstroNet: When Astrocyte Meets Artificial Neural Network. In *Proceedings of the IEEE/CVF Conference on Computer Vision and Pattern Recognition*, 20258–20268.
- Han, Z.; Islam, N.; and Sengupta, A. 2022. Astromorphic Self-Repair of Neuromorphic Hardware Systems. *arXiv preprint arXiv:2209.07428*.
- Haydon, P. G.; and Carmignoto, G. 2006. Astrocyte control of synaptic transmission and neurovascular coupling. *Physiological reviews*, 86(3): 1009–1031.
- Hu, Y.; Wu, Y.; Deng, L.; and Li, G. 2021. Advancing residual learning towards powerful deep spiking neural networks. *arXiv e-prints*, arXiv–2112.
- Huang, J.; Serb, A.; Stathopoulos, S.; and Prodromakis, T. 2023. Text classification in memristor-based spiking neural networks. *Neuromorphic Computing and Engineering*, 3(1): 014003.
- Karimi, G.; Ranjbar, M.; Amirian, M.; and Shahim-Aeen, A. 2018. A neuromorphic real-time VLSI design of Ca²⁺ dynamic in an astrocyte. *Neurocomputing*, 272: 197–203.
- Katharopoulos, A.; Vyas, A.; Pappas, N.; and Fleuret, F. 2020. Transformers are rnns: Fast autoregressive transformers with linear attention. In *International Conference on Machine Learning*, 5156–5165. PMLR.
- Kozachkov, L.; Kastanenko, K. V.; and Krotov, D. 2023. Building transformers from neurons and astrocytes. *Proceedings of the National Academy of Sciences*, 120(34): e2219150120.
- Krizhevsky, A.; and Hinton, G. 2009. Learning multiple layers of features from tiny images.
- Leng, X.-L.; Miao, X.-A.; Liu, T.; et al. 2021. Using recurrent neural network structure with Enhanced Multi-Head Self-Attention for sentiment analysis. *Multimedia Tools and Applications*, 80: 12581–12600.
- Lenk, K.; Satuvuori, E.; Lallouette, J.; Ladrón-de Guevara, A.; Berry, H.; and Hyttinen, J. A. 2020. A computational model of interactions between neuronal and astrocytic networks: the role of astrocytes in the stability of the neuronal firing rate. *Frontiers in computational neuroscience*, 13: 92.
- Li, Y.-X.; and Rinzel, J. 1994. Equations for InsP₃ receptor-mediated Ca²⁺ oscillations derived from a detailed kinetic model: a Hodgkin-Huxley like formalism. *Journal of theoretical Biology*, 166(4): 461–473.
- Liu, J.; Harkin, J.; Maguire, L. P.; McDaid, L. J.; and Wade, J. J. 2017. SPANNER: A self-repairing spiking neural network hardware architecture. *IEEE transactions on neural networks and learning systems*, 29(4): 1287–1300.
- Liu, J.; McDaid, L. J.; Harkin, J.; Karim, S.; Johnson, A. P.; Millard, A. G.; Hilder, J.; Halliday, D. M.; Tyrrell, A. M.; and Timmis, J. 2018. Exploring self-repair in a coupled spiking astrocyte neural network. *IEEE transactions on neural networks and learning systems*, 30(3): 865–875.
- Maas, A. L.; Daly, R. E.; Pham, P. T.; Huang, D.; Ng, A. Y.; and Potts, C. 2011. Learning Word Vectors for Sentiment Analysis. In *Proceedings of the 49th Annual Meeting of the Association for Computational Linguistics: Human Language Technologies*, 142–150. Portland, Oregon, USA: Association for Computational Linguistics.
- Manninen, T.; Aćimović, J.; and Linne, M.-L. 2023. Analysis of network models with neuron-astrocyte interactions. *Neuroinformatics*, 21(2): 375–406.
- Mueller, E.; Studenyak, V.; Auge, D.; and Knoll, A. 2021. Spiking transformer networks: A rate coded approach for processing sequential data. In *2021 7th International Conference on Systems and Informatics (ICSAI)*, 1–5. IEEE.
- Nadkarni, S.; and Jung, P. 2004. Dressed neurons: modeling neural–glial interactions. *Physical biology*, 1(1): 35.
- Nadkarni, S.; and Jung, P. 2007. Modeling synaptic transmission of the tripartite synapse. *Physical biology*, 4(1): 1.
- Navarrete, M.; and Araque, A. 2010. Endocannabinoids potentiate synaptic transmission through stimulation of astrocytes. *Neuron*, 68(1): 113–126.
- Pennington, J.; Socher, R.; and Manning, C. D. 2014. GloVe: Global Vectors for Word Representation. In *Empirical Methods in Natural Language Processing (EMNLP)*, 1532–1543.
- Perez-Catalan, N. A.; Doe, C. Q.; and Ackerman, S. D. 2021. The role of astrocyte-mediated plasticity in neural circuit development and function. *Neural Development*, 16(1): 1–14.
- Polykretis, I.; Tang, G.; and Michmizos, K. P. 2020. An astrocyte-modulated neuromorphic central pattern generator for hexapod robot locomotion on intel’s loihi. In *International Conference on Neuromorphic Systems 2020*, 1–9.
- Radford, A.; Narasimhan, K.; Salimans, T.; and Sutskever, I. 2018. Improving language understanding by generative pre-training.
- Ramachandran, P.; Parmar, N.; Vaswani, A.; Bello, I.; Levskaya, A.; and Shlens, J. 2019. Stand-alone self-attention in vision models. *Advances in neural information processing systems*, 32.
- Ranjbar, M.; and Amiri, M. 2015. An analog astrocyte–neuron interaction circuit for neuromorphic applications. *Journal of Computational Electronics*, 14(3): 694–706.
- Rastogi, M.; Lu, S.; Islam, N.; and Sengupta, A. 2021a. On the Self-Repair Role of Astrocytes in STDP Enabled Unsupervised SNNs. *Frontiers in Neuroscience*, 14: 603796.
- Rastogi, M.; Lu, S.; Islam, N.; and Sengupta, A. 2021b. On the Self-Repair Role of Astrocytes in STDP Enabled Unsupervised SNNs. *Frontiers in Neuroscience*, 14: 1351.
- Rusch, T. K.; and Mishra, S. 2020. Coupled Oscillatory Recurrent Neural Network (coRNN): An accurate and (gradient) stable architecture for learning long time dependencies. *arXiv preprint arXiv:2010.00951*.
- Rusch, T. K.; and Mishra, S. 2021. Unicornn: A recurrent model for learning very long time dependencies. In *International Conference on Machine Learning*, 9168–9178. PMLR.

Schlag, I.; Irie, K.; and Schmidhuber, J. 2021. Linear transformers are secretly fast weight programmers. In *International Conference on Machine Learning*, 9355–9366. PMLR.

Sengupta, A.; Ye, Y.; Wang, R.; Liu, C.; and Roy, K. 2019. Going deeper in spiking neural networks: VGG and residual architectures. *Frontiers in neuroscience*, 13.

Shaw, P.; Uszkoreit, J.; and Vaswani, A. 2018. Self-attention with relative position representations. *arXiv preprint arXiv:1803.02155*.

Srinivasan, G.; Lee, C.; Sengupta, A.; Panda, P.; Sarwar, S. S.; and Roy, K. 2020. Training deep spiking neural networks for energy-efficient neuromorphic computing. In *ICASSP 2020-2020 IEEE International Conference on Acoustics, Speech and Signal Processing (ICASSP)*, 8549–8553. IEEE.

Tsybina, Y.; Kastalskiy, I.; Krivososov, M.; Zaikin, A.; et al. 2022. Astrocytes mediate analogous memory in a multi-layer neuron–astrocyte network. *Neural Computing and Applications*, 34(11): 9147–9160.

Vaswani, A.; Shazeer, N.; Parmar, N.; Uszkoreit, J.; Jones, L.; Gomez, A. N.; Kaiser, Ł.; and Polosukhin, I. 2017. Attention is all you need. *Advances in neural information processing systems*, 30.

Volman, V.; Ben-Jacob, E.; and Levine, H. 2007. The astrocyte as a gatekeeper of synaptic information transfer. *Neural computation*, 19(2): 303–326.

Wade, J.; McDaid, L.; Harkin, J.; Crunelli, V.; and Kelso, S. 2012a. Self-repair in a Bidirectionally Coupled Astrocyte-Neuron (AN) System based on Retrograde Signaling. *Frontiers in Computational Neuroscience*, 6.

Wade, J.; McDaid, L. J.; Harkin, J.; Crunelli, V.; and Kelso, S. 2012b. Self-repair in a bidirectionally coupled astrocyte-neuron (AN) system based on retrograde signaling. *Frontiers in computational neuroscience*, 6: 76.

Wade, J. J.; McDaid, L. J.; Harkin, J.; Crunelli, V.; and Kelso, J. S. 2011. Bidirectional coupling between astrocytes and neurons mediates learning and dynamic coordination in the brain: a multiple modeling approach. *PloS one*, 6(12): e29445.

Wakida, N. M.; Gomez-Godinez, V.; Li, H.; Nguyen, J.; et al. 2020. Calcium dynamics in astrocytes during cell injury. *Frontiers in Bioengineering and Biotechnology*, 8: 912.

Wang, Z.; Zhang, Y.; Shi, H.; Cao, L.; Yan, C.; and Xu, G. 2022. Recurrent spiking neural network with dynamic presynaptic currents based on backpropagation. *International Journal of Intelligent Systems*, 37(3): 2242–2265.

Yang, Y.; and Li, P. 2021. Bioleaf: A bio-plausible learning framework for training of spiking neural networks. *arXiv preprint arXiv:2111.13188*.

Zhou, C.; Yu, L.; Zhou, Z.; Zhang, H.; Ma, Z.; Zhou, H.; and Tian, Y. 2023. Spikingformer: Spike-driven Residual Learning for Transformer-based Spiking Neural Network. *arXiv preprint arXiv:2304.11954*.

Zhou, Z.; Zhu, Y.; He, C.; Wang, Y.; Yan, S.; Tian, Y.; and Yuan, L. 2022. Spikformer: When spiking neural network meets transformer. *arXiv preprint arXiv:2209.15425*.

Supplementary Material

Appendix A: Transformer Illustration

Transformer employs only encoder architecture for performing sentiment classification and vision tasks. As illustrated in Fig. 5, the input embeddings combined with the positional embeddings enter the encoder layer as input tokens. Then *key*, *query* and *value* are generated from the input tokens and after performing self attention on them, a skip connection is added from the inputs and the overall result is layer normalized and fed into a feed forward network. Another add & normalize operation is performed before feeding them into a linear layer and softmax function to obtain the output probabilities. Sometimes, there might be more than one encoder layer. For different tasks, like machine translation and text generation, encoder-decoder or only decoder type architecture of transformer can be used. However, independent of the type of architecture needed, self-attention is a fundamental mechanism defining transformer operation. The “Multi-Head Attention” Block has self-attention modules parallelly running on different heads obtained from the input embeddings.

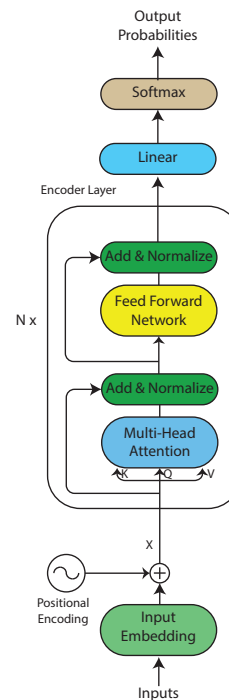


Figure 5: Schematic representation of the Transformer Encoder architecture, illustrating the sequential flow of operations. N denotes the number of encoder layers in the network.

Appendix B: Memory Efficient Linearized Attention

Linearized attention involves utilizing feature maps with lower complexity levels, thereby minimizing memory and

Hyper-parameters	Value	Tested Range
α (Non-linearity parameter)	0.25	0.15-0.4
Model size (D)	128	32-256
(Scaling parameter m)	500D	(1-1000)D
Model size	128	32-256
Sequence length	400	100-600
Learning rate	0.00001	$1e-4 - 1e-6$
Batch size	64	8-256
Number of epochs	120	40-150
Number of heads	4	1-12

Table 2: Hyper-parameter list for the IMDB dataset.

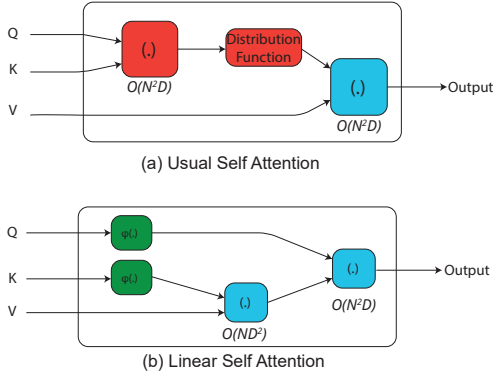


Figure 6: Figure showing the comparison of order of complexity between usual and linearized self-attention. Distribution function can be mapped to softmax function used in usual transformers.

computational resources. As discussed before, the introduction of non-linearity in biological neurons is facilitated by an activation function ($elu(X)$) in the hidden layer neurons. The utilization of the positive similarity feature map, denoted by $\phi(\cdot)$, characterizes the implementation of the linearized attention operation as described in the work by (Katharopoulos et al. 2020). The utilization of linearized feature attention results in a reduction of computational complexity associated with the computation of the attention score. The advantage of utilizing feature map based linearized attention over the conventional distribution function (*i.e.* softmax) based self-attention is demonstrated in Fig. 6.

Usual self-attention employs softmax as the distribution function, however, the dot product of *Query* (Q) and *Key* (K) poses an $O(N^2D)$ complexity which overuses the memory. Whereas, in linearized attention the computation multiplies *Key* (K) and *Value* (V) yielding an $O(ND^2)$ complexity, properly utilizing the memory and computational efficiency when token length (N) is larger than internal embedding size (D). Thus, the employment of the linearized feature map, denoted as $\phi(\cdot)$, enables the realization of memory efficient linearized transformer.

Hyper-parameters	Value	Tested Range
α (Non-linearity parameter)	0.25	0.15-0.4
Model size (D)	256	64-512
(Scaling parameter m)	500D	(1-1000)D
Patch size	2	2-4
Learning rate	0.001	$1e-2 - 1e-4$
Batch size	32	8-128
Number of epochs	250	80-300
Number of heads	8	2-12

Table 3: Hyper-parameter list for the CIFAR10 dataset.

Appendix C: Hyper-parameter Details

The hyper-parameters for the encoder-type astromorphic transformer for the IMDB dataset are listed in Table 2 in the supplementary material. The hyper-parameters for the encoder-type convolution and astromorphic self-attention based transformer for the CIFAR10 dataset are listed in Table 3.